Modeling the magnetostriction effect in elastomers with magnetically soft and hard particles

Electronic supplemental information for Soft Matter

Pedro A. Sánchez Oleg V. Stolbov
Sofia S. Kantorovich Yuriy L. Raikher

In this document we provide further details on two main aspects: first, we detail our considerations on the physical properties of spherical MH particles used experimentally for the creation of HSMEs and discuss how they support our modeling assumptions; second, we present technical details of the bead-spring model and its corresponding simulation protocol.

S1 Considerations on the magneto-mechanical properties of spherical MH particles embedded in an elastic matrix

Typical spherical MH microparticles, as the ones used in HSME samples of Reference [61] of the main manuscript (Magnequench NdFeB), are actually a solid clot of 10^5–10^6 nanograins whose magnetization follows the Stoner-Wohlfarth scenario. They have typical coercive forces of at least 500–700 kA/m (7–9 kOe) and, after being magnetized by an initial external strong field, $\vec{H}_i$, a typical remanence of around $M_R \approx 400$–500 kA/m. Therefore, they behave effectively as monodomain particles with magnetic moment $\|\vec{\mu}_h\| = M_R V$, proportional to their volume, V, so that they can be represented as spheres with a point magnetic dipole $\vec{\mu}_h$ located at their centers. In HSME materials, the magnetization of the sample takes place after all solid particles have been embedded into the polymer matrix. Due to the large amount of nanograins with randomly oriented easy axes forming each embedded MH microparticle, its effective dipole moment essentially points in the direction of the initial magnetizing field, $\vec{H}_i$. That is, all MH particles in the sample have their magnetic moments oriented in the same direction.

Let us examine the response of one of the embedded MH magnetized particles when exposed to a homogeneous external field, H_0, antiparallel to the orientation of its magnetic dipole. We assume that such field is weaker than the coercive force necessary to invert the orientation of the dipole. In order to determine whether the whole particle will rotate to align with the field or not, we take the Hooke torsion expression to represent the elastic energy associated to such rotation:

$$U = \mu H_0 \cos\theta + 3GV\theta^2, \tag{1}$$

where θ is the rotation angle from the initial orientation of the MH particle (that is, $\theta = 0$ for no rotation) and G is the shear modulus of the polymer matrix. Note that the sign of the first term is positive because the field is antiparallel to the actual direction of the magnetic moment of the particle.

Expanding (1) for small angular deviations, one gets

$$U \approx M_R V H_0 \left(1 - \frac{\theta^2}{2} + \frac{\theta^4}{24}\right) + 3GV\theta^2. \tag{2}$$

Differentiation of this elastic energy with respect to θ yields

$$\frac{\partial U}{\partial \theta} \approx -M_R V H_0 \theta + \frac{M_R V H_0}{6}\theta^3 + 6GV\theta, \tag{3}$$

so that the condition for equilibrium between magnetic and elastic components reads

$$\theta\left(6GV - M_R V H_0 + \frac{M_R V H_0}{6}\theta^2\right) = 0. \tag{4}$$

This equation has three roots. One is $\theta = 0$ (no rotation), whereas two others are

$$\theta = \pm\sqrt{6\,(1 - 6G/M_R H_0)}. \tag{5}$$

The sign in (5) is irrelevant, what matters is the non-negativity of the expression under the radical. It requires

$$H \geq H_r \equiv 6G/M_R. \tag{6}$$

Thus, we arrive at the conclusion that at fields lower than H_r the particle is in a stable state and does not rotate. Note that the point $H_0 = H_r$ is a bifurcation: here all the roots of equation (4) coincide and equal zero; at higher fields, angle gradually increases, *i.e.*, the particle begins to rotate.

For a dimensional estimate of the critical field H_r, we set $G = 10^5$ dyn/cm^2 = 10 kPa, that corresponds to a very soft matrix, and take the same value for M_R as above:

$$H_r \approx 6 \cdot 10^5/400 \approx 1.5 \text{ kOe} = 120 \text{ kA/m}. \tag{7}$$

This is not a very strong field but, still, it is by no means a weak one.

With respect to the essence of our paper, the most important question is whether the passage from prolate to oblate aspect ratio of the MS shell occurs at fields weaker

than H_r, $|H_0| < |H_r|$. Otherwise, it would mean that the effect we observe in our models is unphysical. To find that, we convert H_r into our system of reduced units

$$\tilde{H}_r = H_r/\sqrt{G} \approx -1500/\sqrt{10^5} \approx -4.7. \tag{8}$$

Comparison of this value with the fields sampled in Figure 6 of the main text proves that, under the assumptions made (and they are not at all unreal), the predicted effect should be observable. In addition, experimental evidence supports this conclusion. Let us look at Figure 4b from Reference [YY] in the main text. As it shows, in the interval [100,0] kA/m the magnetization curves of very soft composites (sample S2, Young modulus 36 kPa, shear modulus 12 kPa, cf. our 10 kPa) and that of the entirely solid composite (epoxy, shear modulus many orders of magnitude greater) are very close. This means that the compliance of the matrix does not have any significant effect on the behavior of samples under moderately negative fields, provided that the compared materials had been initially magnetized by the same field.

S2 Details of the MD simulation protocol

Note that all magnitudes mentioned below are expressed in the system of reduced units introduced in the main text.

In Langevin dynamics simulations, the translational and rotational equations of motion acting on each particle i are defined as

$$\begin{aligned} m_i(d\vec{v}_i/dt) &= \vec{F}_i - \Gamma_{\mathrm{T}}\vec{v}_i + \vec{\xi}_{i,\mathrm{T}}, \\ \vec{I}_i \cdot (d\vec{\omega}_i/dt) &= \vec{\tau}_i - \Gamma_{\mathrm{R}}\vec{\omega}_i + \vec{\xi}_{i,\mathrm{R}}, \end{aligned} \tag{9}$$

where $\vec{F}_i$ and $\vec{\tau}_i$ are the total force and torque, m_i is the particle mass and $\vec{I}_i$ its inertia tensor, Γ_{T} and Γ_{R} the translational and rotational friction constants, and $\vec{\xi}_{i,\mathrm{T}}$ and $\vec{\xi}_{i,\mathrm{R}}$ are a Gaussian random force and torque, respectively, fulfilling the usual fluctuation-dissipation rules,

$$\begin{aligned} \langle \xi(t) \rangle &= 0, \\ \langle \xi_i(t)\xi_j(t') \rangle &= 6T\Gamma\delta_{ij}\delta(t-t'). \end{aligned} \tag{10}$$

Since in this study we are not interested in the system dynamics but only on static structural properties after magnetomechanical relaxation, the values of the friction constants can be chosen arbitrarily, as long as they provide a fast system relaxation. In general, we use $\Gamma_{\mathrm{R}} = \Gamma_{\mathrm{T}}/3$.

In order to place N_s MS particles inside a shell around the central MH particle, we set a temporary steric spherical wall of radius d_h concentric to the latter. The MS particles are then allocated randomly with respect to the MH one at center-to-center distances $d_h/2 < r < d_h$. This random initial configuration is relaxed by performing 3 damped dynamics simulation cycles of $2 \cdot 10^3$ integration steps each, using as time step $\delta t = 5 \cdot 10^{-3}$, at $T = 0.1$. In such cycles, only steric interaction are considered, Γ_{T} is decreased from 10 to 1 and the maximum force allowed in the system is slowly

increased. After this, another cycle of 10^4 damped integation steps is performed under $T = 0.001$, $\Gamma_{\mathrm{T}} = 10$ and no force limitation.

Once the initial confined relaxation is completed, the temporary spherical shell is removed and the crosslinking procedure takes place according to the positions of the MS particles. After the spring network is defined, three additional simulation cycles are carried out. The first consists of 10^4 integration steps, with $T = 0.01$ and $\Gamma_{\mathrm{T}} = 15$. Then, dipole-dipole interactions start to be taken into account and a second cycle of 10^4 integration steps at $T = 0.001$ and $\Gamma_{\mathrm{T}} = 10$ is performed. Finally, the value of the external applied is set and a final integration of 10^6 steps, with $\Gamma_{\mathrm{T}} = 10$, is completed. Only the final configuration from each independent run is analyzed.

S3 Distribution of spring elastic constants

In our spherical shell network system, the assignation to each spring of an elastic constant proportional to its equilibrium length provides a rather linear distribution of values, as can be seen in the example of Figure S3.1.

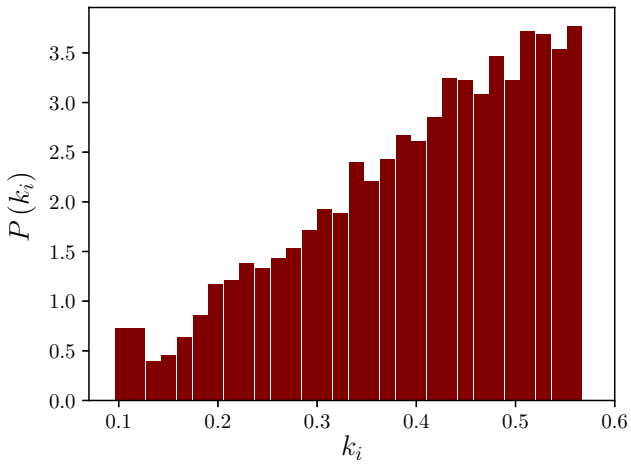

Figure S3.1: Example of distribution of elastic constants used in a simulation run with $\bar{k} = 0.4$.

S4 Fitting of the elastic properties of the simulation model

Figure S4.1 shows some examples of the comparison performed between the results of continuum and bead-spring models in order to fit the average spring elastic constant, $\bar{k}$, in the latter. Note that $\bar{k} = 0.4$ provides the best match.

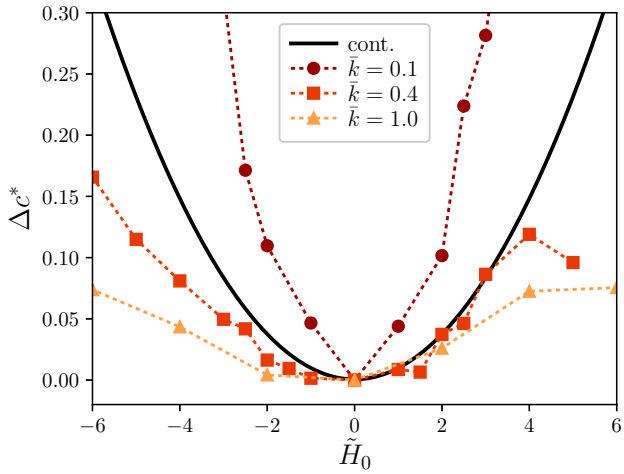

Figure S4.1: Longitudinal deformation parameter, Δc^*, as a function of the applied field, $\tilde{H}_0$, obtained when the MH particle is not magnetized, $\tilde{\mu}_h = 0$: solid line corresponds to the continuum model, symbols to simulation results of the bead-spring model under different values of the average spring constant, $\bar{k}$.